

1 Dear Siv Lauvset,

2

3 I have now received the reviewers reports on the revised version of your paper. As you will find,
4 one reviewer has still a small problem with the calculation of the available light for the off-line
5 calculations. It would be ideal if you could rerun the off-line calculations following the
6 reviewers suggestion, and check if/how much this changes your conclusions.

7

8 **Reply: Thank you for your comments. I have done the additional calculation the reviewer asks for**
9 **and find that there is no change (see also my reply to reviewer #2 below). I have added one**
10 **sentence to this effect (explaining that attenuating light to 50m is equivalent to using an average**
11 **over the 100m).**

12

13 In addition, I have a few additional suggestions:

14

15 in Eq. 1, N_0 is not defined

16

17 In 169 insert 'mean' after 'zonal'

18

19 In 172 emissions 'of'

20

21 In 173 I suggest to put 'accumulation mode' in quotes

22 or add the diameter in parenthesis as not many readers of BG might be familiar with the term
23 also: ...emissions...'were' increased

24

25 In 174 allowing 'for' the full interactive cycle

26 (or 'allowing the simulation of' the full...)

27

28 In 200 global mean SST 'is' projected

29

30 In 213 oxygen is not a physical variable...

31 perhaps 'physically driven, such as surface oxygen' is meant?

32

33 In 223 the spatial 'distribution of' the absolute change in SST...

34

35 In 226-228 I'm a bit puzzled how one can see the 'changes in spatial patterns'

36 in the zonal means figure. Perhaps this can be clarified.

37

38 In 300 All RM 'experiments' (not methods) also exhibit...

39

40 In 314/315 I suggest to change the sentence to

41 ...it takes less than five years for ocean NPP to decrease to RCP8.5 levels.

42

43 In 346 ...upwelling regions (add 's')

44

45 In 690 Journal of 'C'limate

46

47 **Reply: All the changes suggested above have been implemented. With the exception of changing**

48 “methods” to “experiments” on line 300. “Methods” is the word used throughout the manuscript
49 and we feel that it is more appropriate to keep it consistent.

Report #1

Anonymous Referee #2

The manuscript has basically taken into account all my criticisms from my first review, so I would argue to publish it. There is only one minor point: For the offline calculations, the authors use the incident light attenuated to a depth of 50m. Unlike the nutrients, or the biomass, which are averaged over the upper 100m for the offline calculations, this is not a true average; but calculating an average would probably be easy: average attenuation could be calculated from $k = k_{\text{water}} + k_{\text{chl}} * \text{Chl}$ and then the average light could be calculated from

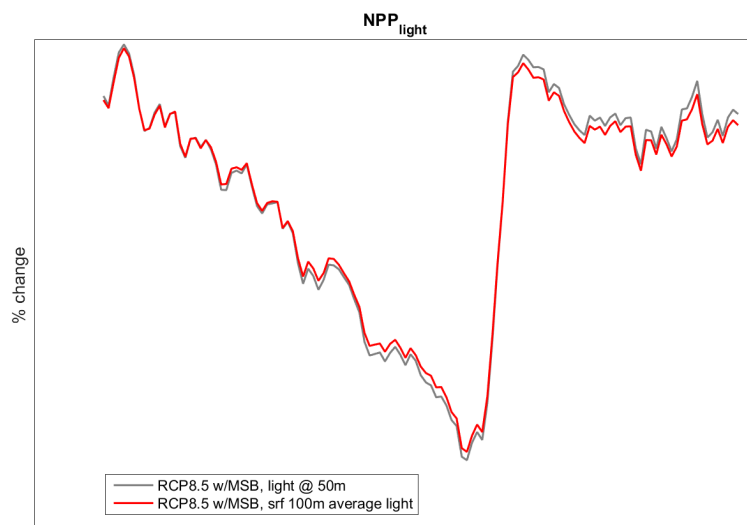
$$I_{\text{av}} = 1/100m * \int_{0}^{100m} I(z=0) * \exp(-k*z) dz$$

I don't expect this to change the main conclusions crucially, but it might give a somewhat different residual NPP as calculated with $I(z=50m)$, and thus a slightly different conclusion about the role of nutrients. Maybe the authors could quickly check that. I don't think it would take too much time.

Otherwise the paper is fine now and I would recommend publication.

50

51 **Reply: The light is attenuated by a different equation in the model so we have used that also in our**
52 **offline calculations. I have previously looked at results obtained when the light is not attenuated at**
53 **all, and this has a small effect. Using average light (over the top 100m) is not significantly different**
54 **from using light attenuated to 100m. The figure below shows the NPP_{light} component for the**
55 **marine sky brightening experiment with two different light attenuations (time on the x-axis). The**
56 **other experiments show similar differences.**



57

58 **Climate engineering and the ocean: effects on biogeochemistry and primary production**

59 Siv K. Lauvset¹, Jerry Tjiputra¹, Helene Muri²,

60 ¹Uni Research Climate, Bjerknes Center for Climate Research, Jahnebakken 5, Bergen,

61 Norway

62 ²University of Oslo, Department of Geosciences, Section for Meteorology and Oceanography,

63 Oslo, Norway

64

65 **ABSTRACT**

66 Here we use an Earth System Model with interactive biogeochemistry to project future ocean

67 biogeochemistry impacts from large-scale deployment of three different radiation

68 management (RM) climate engineering (also known as geoengineering) methods:

69 stratospheric aerosol injection (SAI), marine sky brightening (MSB), and cirrus cloud

70 thinning (CCT). We apply RM such that the change in radiative forcing in the RCP8.5

71 emission scenario is reduced to the change in radiative forcing in the RCP4.5 scenario. The

72 resulting global mean sea surface temperatures in the RM experiments are comparable to

73 those in RCP4.5, but there are regional differences. The forcing from MSB, for example, is

74 applied over the oceans, so the cooling of the ocean is in some regions stronger for this

75 method of RM than for the others. Changes in ocean net primary production (NPP) are much

76 more variable, but SAI and MSB give a global decrease comparable to RCP4.5 (~6% in 2100

77 relative to 1971-2000), while CCT give a much smaller global decrease of ~3%. Depending

78 on the RM methods, the spatially inhomogeneous changes in ocean NPP are related to the

79 simulated spatial change in the NPP drivers (incoming radiation, temperature, availability of

80 nutrients, and phytoplankton biomass), but mostly dominated by the circulation changes. In

81 general, the SAI and MSB - induced changes are largest in the low latitudes, while the CCT -

82 induced changes tend to be the weakest of the three. The results of this work underscores the
83 complexity of climate impacts on NPP, and highlights that changes are driven by an
84 integrated effect of multiple environmental drivers, which all change in different ways. These
85 results stress the uncertain changes to ocean productivity in the future and advocates caution
86 at any deliberate attempt for large-scale perturbation of the Earth system.

87

88 **1 INTRODUCTION**

89 Human emissions of carbon dioxide to the atmosphere is unequivocally causing global
90 warming and climate change (IPCC, 2013). At the 21st United Nations Framework
91 Convention on Climate Change (UNFCCC) Conference of the Parties, it was agreed to limit
92 the increase in global mean temperature to 2°C above pre-industrial levels and to pursue
93 efforts to remain below 1.5°C. Reaching this goal will not be possible without radical social
94 transformation. Solar radiation management (SRM) has been suggested as both a method of
95 offsetting global warming and to reduce risks associated with climate change, substituting
96 some degree of mitigation (Teller et al., 2003, Bickel and Lane, 2009), or to buy time to
97 reduce emissions (Wigley, 2006). Reducing the otherwise large anthropogenic changes in the
98 marine ecosystem drivers (*e.g.*, temperature, oxygen, and primary production) could also be
99 beneficial for vulnerable organisms that need more time to migrate or adapt (Henson et al.,
100 2017). SRM is the idea to increase the amount of solar radiation reflected by Earth in order to
101 offset changes in the radiation budget due to the increased greenhouse effect from
102 anthropogenic emissions, *i.e.* a form of climate engineering – or geoengineering.

103 Here we have performed model experiments with stratospheric sulfur aerosol
104 injections (Crutzen, 2006; Weisenstein et al., 2015), marine sky brightening (Latham, 1990),
105 and cirrus cloud thinning (Mitchell and Finnegan, 2009) applied individually. Stratospheric
106 aerosol injections (SAI) would involve creating a layer of reflective particles in the

107 stratosphere to reduce the amount of solar radiation reaching the surface. The most widely
108 discussed approach to SAI is to release a gaseous sulfate precursor, like SO₂, which would
109 oxidize to form sulfuric acid and then condensate to reflective aerosol particles (e.g. Irvine et
110 al. 2016). Marine sky brightening (MSB) aims to reflect the incoming solar radiation at lower
111 levels in the atmosphere. Here, the idea is to spray naturally occurring sea salt particles into
112 low-lying stratiform clouds over the tropical oceans to increase the available cloud
113 condensation nuclei, thus increasing the concentration of smaller cloud droplet and increase
114 the reflectivity of the clouds (Latham, 1990). The sea salt aerosols are reflective in themselves
115 (e.g., Ma et al., 2008), adding to the cooling potential of the method. Cirrus cloud thinning
116 (CCT) on the other hand, aims to increase the amount of outgoing longwave radiation at the
117 top of the atmosphere. This is envisioned done by depleting the longwave trapping in high ice
118 clouds by seeding them with highly potent ice nuclei (e.g., Mitchell and Finnegan, 2009;
119 Storelvmo et al., 2013). In the absence of naturally occurring ice nuclei, the seeded material
120 would facilitate freezing at lower supersaturations, enabling the growth of fewer and larger
121 ice crystals. These would eventually grow so large that they sediment out of the upper
122 troposphere reducing the lifetime and optical thickness of the cirrus clouds leading to a
123 cooling effect. Together these three methods are referred to as Radiation Management (RM).

124 As pointed out by Irvine et al. (2017), there are several gaps in the research on the
125 impact of RM on both global climate and the global environment, especially considering that
126 only a few modelling studies to date systematically compare multiple RM methods. Aswathy
127 et al. (2015) and Niemeier et al. (2013) compared stratospheric sulfur aerosol injections to
128 brightening of marine clouds in terms of the hydrological cycle and extremes in temperatures
129 and precipitation. Crook et al. (2015) compared the three methods used in this study, but
130 restricted the study to temperatures and precipitation. This study focuses on the impact on the
131 ocean carbon cycle, which could feedback to climate (Friedlingstein et al., 2006), and in

132 particular on ocean primary production (NPP), which is known to be temporally and spatially
133 complex.

134 The effect RM has on the ocean carbon cycle and ocean productivity has been studied
135 previously, but limited to the use of simple one-dimensional models (Hardman-Mountford et
136 al., 2013) or with global models but focusing on a single method of RM (Partanen et al.,
137 2016; Tjiputra et al., 2016, Matthews et al., 2009). Due to the many uncertainties and open
138 questions associated with RM impacts, a systematic comparative approach is necessary. The
139 three different methods of RM used in this study are likely to have different effects on both
140 the climate and the ocean, due to the differences in the type of forcing being applied. A
141 concern of RM is that it may allow for continued CO₂ emissions in the future without the
142 accompanied temperature increases and that it does not directly affect the atmospheric CO₂
143 concentrations. Ocean acidification, a direct consequence of increased CO₂ concentrations in
144 the atmosphere, would therefore continue with RM, unless paired with mitigation and / or
145 carbon dioxide removal (CDR).

146 This manuscript is the first to evaluate and compare the effect and impact of multiple
147 RM techniques on ocean biogeochemistry using a fully coupled state-of-the-art Earth system
148 model, and furthermore extends previous studies by looking into impacts introduced by three
149 different large-scale RM deployment scenarios both during and after deployment periods. It is
150 also the first study to assess the impacts of cirrus cloud thinning on ocean biogeochemistry.
151 Our focuses are on impacts on sea surface temperature (SST), oxygen, pH, and NPP, which
152 are the four climate drivers identified by the Intergovernmental Panel on Climate Change
153 (IPCC), significantly affecting marine ecosystem structure and functioning. In a wider
154 perspective, ocean NPP is often used as an indicator for marine food availability, such as
155 fisheries, so furthering our understanding has direct societal implications and a strong
156 connection to the United Nations Sustainable Development Goals.

157 The model and experiments are described in detail in Section 2, the impacts on ocean
158 temperature, oxygen content, the inorganic carbon cycle, and NPP are presented and
159 discussed in Section 3, in addition to a comparison of our results to previous studies, while
160 Section 4 summarizes and concludes the study.

161

162 **2 METHODS**

163 **2.1 Model description**

164 Three RM methods were simulated using the Norwegian Earth System Model
165 (NorESM1-ME; Bentsen et al., 2013). The NorESM1-ME is a fully coupled climate-carbon
166 cycle model, which has contributed to the fifth assessment of the IPCC and participated in
167 numerous Coupled Model Intercomparison Project phase 5 (CMIP5) analyses. For a full
168 description of the physical and carbon cycle components of the model, the readers are referred
169 to Bentsen et al. (2013) and Tjiputra et al. (2013), respectively. Here, we only briefly describe
170 some key processes in the ocean carbon cycle that are relevant for this study.

171 The ocean carbon cycle component of the NorESM1-ME originates from the Hamburg
172 Oceanic Carbon Cycle Model (HAMOCC; Maier-Reimer et al., 2005). In the upper ocean,
173 the lower trophic ecosystem is simulated using an NPZD-type (Nutrient-Phytoplankton-
174 Zooplankton-Detritus) module. The NPP depends on phytoplankton growth and nutrient
175 availability within the euphotic layer (for some of our calculations assumed to be 100 m). In
176 addition to multi-nutrient limitation, the phytoplankton growth is light- and temperature-
177 dependent. The NPP in NorESM1-ME is parameterized using the equations of Six and Maier-
178 Reimer (1996) (Equation 1).

$$179 \quad G = r(T, L) * \frac{N}{N+N_0} \quad \text{Equation 1}$$

180 Where G is the growth rate and

$$181 \quad r(T, L) = \frac{f(L) * f(T)}{\sqrt{(f(L)^2 + f(T)^2)}} \quad \text{Equation 2}$$

182 N is the concentration of the limiting nutrient (either phosphate, nitrate or dissolved iron), N_0
183 is the half-saturation constant for nutrient uptake, $f(L)$ is the function determining light-
184 dependency, and $f(T)$ is the function for temperature-dependency. Both $f(L)$ and $f(T)$ were
185 defined in Six and Maier-Reimer (1996).

$$186 \quad NPP = G * P \quad \text{Equation 3}$$

187 NPP is the net primary production and P is the phytoplankton concentration.

188 In addition to the growth through NPP, the phytoplankton has several sink terms due
189 to mortality, exudation, and zooplankton grazing. All nutrients, plankton, and dissolved
190 biogeochemical tracers are prognostically advected by the ocean circulation. The model
191 adopts generic bulk phytoplankton and zooplankton compartments. The detritus is divided
192 into organic and inorganic materials: particulate organic carbon, biogenic opal, and
193 calcium carbonate. Organic carbon, once exported out of the euphotic layer, is remineralized
194 at depth – a process that consumes oxygen in the ocean interior. Non-remineralized particles
195 reaching the seafloor undergo chemical reactions with sediment pore water, bioturbation, and
196 vertical advection within the sediment module. The model calculates air-sea CO₂ fluxes as a
197 function of seawater solubility, gas transfer rate, and the gradient of the gas partial pressure
198 (pCO₂) between atmosphere and ocean surface, following Wanninkhof (1992). Prognostic
199 surface ocean pCO₂ is computed using inorganic seawater carbon chemistry formulation
200 following the Ocean Carbon-cycle Model Intercomparison Project (OCMIP2).

201 In this study, we made use of ocean NPP simulated by the NorESM1-ME (hereafter
202 referred to as “online calculations”), as well as calculations using the monthly averaged model

203 outputs (hereafter referred to as “offline calculations”). The offline calculations also made use
204 of Equations 1-3, same as the model, but unlike in the model (i), the average value over the
205 top 100 m was used for N , T , and P alike; (ii) L was approximated as incident light at surface
206 attenuated to a constant depth of 50 m; (iii) the monthly mean was used for N , T , L , and P .

207 The choice of attenuation depth for the light has a small, but not significant, effect on the
208 results. Averaging the light input over the top 100 m does, however, yield the same results as
209 using an attenuation depth of 50 m. The offline calculations allowed us to decompose and
210 identify the dominant drivers for the simulated changes. The decomposition was done by
211 choosing to keep all but one parameter, x , constant at a time to quantify the contribution of x
212 to the total change. Table 1 describes how this was done. The parameters being kept constant
213 were kept at the long-term (80 year) monthly mean, as calculated from the pre-industrial
214 model experiment (with constant atmospheric CO₂ concentrations).

215

216 **2.2 Experiment setup**

217 SAI, MSB, and CCT were applied individually to the RCP8.5 (Representative
218 Concentration Pathway) future scenario (Table 2). The target of the simulations were to
219 reduce the global mean top of the atmosphere (TOA) radiative flux imbalance of RCP8.5
220 down to RCP4.5. In each experiment, the forcing is applied over the years 2020 to 2100. To
221 study the termination effect, the simulations were continued for another 50 years following
222 the cessation of each RM method. Here, the SAI, MSB, and CCT experiments are analyzed
223 and compared to the RCP4.5 and RCP8.5 scenarios (Riahi et al., 2011; Thomson et al., 2011)
224 (Table 2). All simulations were run with interactive biogeochemistry and used prescribed
225 anthropogenic CO₂ emissions. The atmospheric CO₂ concentrations are therefore
226 prognostically simulated accounting for land-air and sea-air CO₂ fluxes.

227 As the NorESM1-ME model does not include an interactive aerosol scheme in the
228 stratosphere, the dataset of Niemeier and Timmreck (2015) was used to implement the SAI.
229 The stratospheric zonal mean-sulfate aerosol extinction, single scattering albedo and
230 asymmetry factors resulting from SO₂ injections in the tropics were prescribed such that the
231 prescribed aerosol layer in year 2100 correspond to an SO₂ injection strength of 40 Tg SO₂ yr⁻¹
232 (Muri et al., 2017). The MSB follows the method of Alterskjær et al. (2013), where the
233 emissions of ~~an~~ “accumulation mode” sea salt ~~were~~as increased over the oceans. Here we chose
234 to apply this to a latitude band of ±45°. The tropospheric aerosol scheme is fully prognostic,
235 thus allowing for the full interactive cycle with clouds and radiation. As for the CCT, we
236 adopted the approach of Muri et al. (2014), where the terminal velocity of ice crystals at
237 typical cirrus forming temperatures of colder than -38 °C is increased. The maximum
238 effective radiative forcing was found to be limited at about -3.8 W m⁻² for CCT, resulting in a
239 somewhat higher top of the atmosphere (TOA) radiative flux imbalance in this simulation at
240 2100 compared to the other simulations, where an effective radiative forcing of -4.0 W m⁻² in
241 2100 was reached.

242

243 **3 RESULTS AND DISCUSSION**

244 **3.1 Global changes in ocean temperature and oxygen concentration**

245 Relative to the 1971-2000 historical period, the ocean oxygen content in the 200-600
246 m depth interval is projected to decrease by ~6% globally in 2100 in RCP8.5 (Figure 1a). In
247 RCP4.5 on the other hand, the oxygen inventory in the 200-600 m interval shows only a
248 minor decrease of 2% by 2100 (Figure 1a). This difference stems partly from lower oxygen
249 solubility as the ocean warms and partly from changes in ocean stratification and circulation
250 (not shown). When applying RM to RCP8.5, the oxygen concentration in this depth interval
251 follows the RCP4.5 development closely for all three RM methods (ranging from 2-2.6%

252 decrease in 2100 compared to the 1971-2100 average). There are, however, differences
253 between the methods, with SAI yielding slightly larger decreases after 2060 (Figure 1a). After
254 termination of RM, the rate of oxygen reduction accelerates rapidly for the first ten years,
255 before stabilizing at a new rate of decrease of similar magnitude to that in RCP8.5. The
256 projected oxygen reductions do not drop as low as in RCP8.5 after termination of the RM
257 during our simulation period, but had the simulations been continued for some further
258 decades, the oxygen levels would most likely have converged to the RCP8.5 levels. In 2150,
259 RCP8.5 shows a global mean oxygen decrease globally of 9.5%, while the simulations with
260 terminated RM show a global mean oxygen decrease of 8-8.5% (Figure 1a).

261 In RCP8.5, the global mean SST ~~isare~~ projected to increase by ~ 2.5 °C by 2100
262 relative to 2010 (Figure 1b), and ~ 3 °C relative to the 1971-2000 average. With RM, the
263 changes in SST are kept similar to RCP4.5, with an increase ranging from 0.8 to 1.1 °C over
264 the time period between 2020 (start of RM deployment) and 2100 (end of RM deployment).
265 After termination, there is a very rapid SST increase in the subsequent decade before the SST
266 increases more gradually towards that in RCP8.5. Similar to the development in oxygen
267 content, the absolute change in SST in the model runs with terminated RM is still smaller than
268 the absolute change in RCP8.5 (Figure 1b) in 2150. This is mainly due to the slow response
269 time of the ocean, so the SST would eventually converge had the simulations been carried out
270 for a longer period of time after termination. It should be noted that all methods of RM used
271 in this study have been implemented to produce the global mean radiative forcing at the end
272 of the century that is equivalent to offsetting the difference in the anthropogenic radiative
273 forcing between RCP8.5 and RCP4.5, *i.e.* -4 W m^{-2} . This means that the globally averaged sea
274 surface temperature changes, and changes in large-scale physically driven variables such as
275 oxygen, are expected to be close to those in RCP4.5. The results presented here imply that
276 applying RM does not prevent the long-term impacts of climate change, which is also not

277 expected as long as CO₂ emissions are not simultaneously reduced, but would on average
278 delay them. In the case of oxygen concentrations in the 200-600 m depth interval, the changes
279 incurred in RCP4.5 as well as when the three different methods of RM are applied, are mostly
280 not significantly different from the 1971-2000 average (*i.e.* they are smaller than one
281 standard deviation of the 1971-2000 mean, Figure 2). There are a few exceptions where the
282 oxygen changes are significant. These regions, however, highlight how differently the RM
283 methods affect the ocean.

284 The spatial distribution of absolute change in SST in 2071-2100 relative to 1971-2000
285 is shown in Figure 3b for RCP8.5 and Figure 3c for RCP4.5. The changes are significantly
286 smaller in RCP4.5, but the spatial variations are the same in RCP8.5 and RCP4.5. When
287 applying RM, the changes in SST are everywhere smaller than in RCP8.5 at the end of the
288 century. Similar to thermocline oxygen, the spatial-patternsSST changes are altered in some
289 regions, as seen in the zonally averaged temperature changes (Figure 3a). The SAI method
290 yields the temperature change most similar to that in RCP4.5, which is also mirrored in the
291 near surface air temperatures (Muri et al., 2017). MSB yields the SST changes that are most
292 different compared to RCP4.5. For this method there is a strong bimodal pattern in the SST
293 changes in the North Pacific (Figure 3e), which is also seen in oxygen (Figure 2e). The
294 tropical and subtropical changes in SST with MSB are linked to an enhancement of the
295 Pacific Walker cell, which is induced when MSB is applied, which has been found in
296 previous studies such as Bala et al. (2011), Alterskjær et al. (2013), Ahlm et al. (2017), Stjern
297 et al. (2017), and Muri et al. (2017).

298 Regardless of the RM method, some regions, in particular the northwestern Pacific,
299 will still experience levels of warming (cooling) and oxygen loss (gain) exceeding those in
300 RCP4.5. With SAI, the North American west coast, an important region for aquaculture, will,
301 for example, experience enhanced deoxygenation, which is not projected to happen in

302 RCP4.5. The large spatial heterogeneity in how RM affects ocean temperatures and oxygen
303 concentrations highlights that RM can still lead to similar, albeit weaker, detrimental
304 conditions regionally even if beneficial in the global mean.

305

306 **3.2 Global changes in the inorganic ocean carbon cycle**

307 The atmospheric CO₂ concentration continues to rise in all experiments in which RM
308 is applied at similar rate as in RCP8.5 (Figure 4a), given no simultaneous mitigation efforts in
309 these cases. The atmospheric CO₂ concentration in 2100 in RCP8.5 is 1109 ppm and in 2150
310 it is 1651 ppm. In 2100 there is a minor reduction in CO₂ concentrations when RM is applied
311 of 13 -21 ppm compared to RCP8.5, depending on method. MSB gives the largest decrease in
312 atmospheric CO₂. The termination of RM does not significantly affect the atmospheric CO₂
313 evolution and in 2150 there is a marginal reduction of -15 to -26 ppm depending on method,
314 again with MSB giving the largest reduction. The reductions in atmospheric CO₂
315 concentrations when applying RM are due to the decreasing ocean temperatures leading to
316 larger air-sea flux of CO₂ (Figure 4b). Note that the land carbon sinks also increase slightly
317 when RM is applied (Tjiputra et al., 2016, Muri et al., 2017). The lower CO₂ concentration
318 with MSB is due to the forcing from MSB being applied over the oceans, and the cooling of
319 the ocean in many regions thus being stronger for this method of RM (Figure 3e).

320 While RM leads to a small increase in global mean oceanic CO₂ uptake from the
321 atmosphere, due to increased solubility, the difference introduced by each method is not
322 outside of the interannual variability of RCP8.5 up to 2075. By 2100, the different RM
323 methods give an additional CO₂ uptake of ~0.5 PgC yr⁻¹. After termination, the uptake
324 anomaly quickly drops and returns to the same level as RCP8.5 within only two years. Future
325 surface ocean pH is forced by the increasing atmospheric CO₂ concentrations, which drive the

326 uptake of CO₂ in the surface ocean. Thus RM could possibly worsen future ocean
327 acidification, unless atmospheric CO₂ concentrations are dealt with. However, given the small
328 changes in both atmospheric concentrations and ocean uptake stemming from RM, the surface
329 pH is not greatly affected by RM (Figure 4c). Hence, termination does not considerably affect
330 the pH decrease on the surface ocean.

331 Anthropogenic changes in the ocean inorganic carbon content comes from the top
332 down, so it takes a long time for these changes to be observable in the deep ocean. Therefore,
333 the globally averaged deep ocean (>2000 m) pH changes by only 0.06 pH units between 2010
334 and 2150 in RCP8.5 (Figure 4d). The only region where pH changes significantly in the deep
335 ocean is the North Atlantic north of 30°N, where the strong overturning circulation brings
336 anthropogenic carbon to great depths in a relatively short timeframe. Here there is a
337 significant decrease in deep ocean pH between 2010 and 2150 in RCP8.5, as well as the three
338 RM cases (Figure 4e). In RCP8.5, the pH is projected to decrease by ~0.2 pH unit in 2100.
339 RM leads to an additional acidification of 0.02-0.045 (depending on the method of RM) in the
340 deep North Atlantic Ocean, which is large enough to marginally, but not significantly, affect
341 the global average (Figure 4d). A similar result was found by Tjiputra et al. (2016). After
342 termination of RM, the pH keeps decreasing – now at a rate comparable to RCP8.5. This
343 change in rate of decrease after termination happens within ~10 years, indicating that the
344 changes in the inorganic carbon cycle are very quick in the North Atlantic. Both the rapid
345 decrease of deep ocean pH in this region and the rapid recovery towards RCP8.5 development
346 after termination of RM, are likely linked to changes in the Atlantic Meridional Overturning
347 Circulation due to climate change and RM (not shown, see Muri et al., 2017). While the
348 global mean pH below 2000m in RM experiments rebound to that of the RCP8.5, this is not
349 the case for the North Atlantic. In the latter, all RM methods lead to and remain at lower pH

350 than the RCP8.5 by 2150. It is possible that the deep pH in the North Atlantic would recover
351 to that in RCP8.5 had the simulations been continued for another few decades.

352

353 **3.3 Global changes in ocean NPP**

354 The direct effects of RM on surface shortwave radiation and temperature directly
355 affect photosynthesis through the light and temperature dependence of the phytoplankton
356 growth rate. The ocean productivity, and by extension ocean biological carbon pump, is thus
357 indirectly affected by RM. There is a lot of interannual variability in the NPP changes hence
358 Figure 5 shows the 5-year running averages of relative changes to the 1971-2000 average. In
359 RCP8.5, there is a decrease in global NPP of ~10% by 2100 (Figure 5), which is within the
360 range of the decrease projected by CMIP5 models of $-8.6 \pm 7.9\%$ (Bopp et al., 2013) and
361 mainly due to the overall warming leading to a more stratified ocean where there are less
362 nutrients available in the euphotic zone. All RM methods also exhibit decreases in ocean
363 NPP, but the decrease is never as strong as that in RCP8.5. The shortwave-based methods,
364 *i.e.*, SAI and MSB, which reduce the amount of downward solar radiation at the surface, have
365 the largest decreases (~6% in 2100) of the RM methods, which is a stronger decrease than in
366 RCP4.5. The longwave-based CCT method, however, yields only a minor decrease of ~3% in
367 2100, *i.e.* less than in RCP4.5. As the cirrus clouds are thinned or removed, more sunlight
368 reaches the surface ocean, thus promoting and increasing NPP above the RCP4.5 levels.

369 The fact that CCT shows a significant global increase in ocean NPP relative to RCP8.5
370 and even an increase relative to RCP4.5 is a very interesting result of this study. It suggests
371 that when considering the global ocean NPP changes alone, implementation of CCT may
372 offer the least negative impact of the three tested methods. The side effect, however, is that if
373 terminated suddenly at a large-scale deployment with no simultaneous mitigation or CDR

374 efforts, the CCT method would lead to the most drastic change in NPP over very short period.
375 The divergence between methods is particularly strong in the period 2070-2100, as the
376 radiative forcing by RM approaches -4 Wm^{-2} . After termination, it takes less than five years
377 ~~for the ocean NPP to return to RCP8.5 levels again~~
378 ~~for the development of ocean NPP to~~
379 ~~return to RCP8.5 levels again.~~ This is consistent with the rapid warming seen after
379 termination (Figure 1b), and is driven by the fast atmospheric response to the termination.

380 On average there are some interesting spatial features in how NPP changes. Figure 6a
381 shows the zonally averaged difference between 2071-2100 and 1971-2000. In the Northern
382 Hemisphere, NPP decreases everywhere, and decreases less in RCP4.5 and with RM than in
383 RCP8.5. In the Southern Hemisphere, on the other hand, the changes in NPP are much more
384 spatially variable, and the response to the different methods of RM is more variable. Between
385 the Equator and 40°S there is a reduction in NPP in 2071-2100 relative to 1971-2000, while
386 south of 40° there is generally an increase (except in a narrow band at 60°S). In the Southern
387 Hemisphere the impact of CCT is quite different from the impact of SAI and MSB. This is
388 probably due to the change in radiative balance, which is much stronger for CCT in the
389 southern high latitudes than for the other methods (not shown, see Muri et al., 2017). Because
390 of the large spatial and inter-annual variability, the changes incurred to ocean NPP in the
391 future are frequently not significantly different from the 1971-2000 average (*i.e.* the absolute
392 change is smaller than one standard deviation of the 1971-2000 mean, Figure 6b-f). This
393 means that when RM is applied, the ocean NPP does not change in most of the ocean.
394 However, it is clear that the changes in NPP in 2071-2100 relative to 1971-2000 are smaller
395 in RCP4.5 than in RCP8.5 (Figures 6b and 6c), and that the spatial variations in all
396 experiments mainly come from the nutrient availability (not shown), which is furthermore
397 dependent on ocean stratification. There are also some regions of significant change in ocean
398 NPP, which are discussed further in Section 3.5.

400 3.4 Drivers of global changes in ocean NPP

401 To further evaluate how RM affects ocean NPP, we have made offline calculations
402 using Equations 1-3. From the NorESM1-ME model outputs we used the monthly mean
403 nitrate, phosphate, iron, and phytoplankton concentration over the top 100 m, average
404 temperature in the top 100 m, and shortwave radiation input attenuated to 50 m depth. The
405 resulting offline NPP is therefore an approximation of the NPP in the top 100 m of the ocean.
406 The offline global average is 75% of the full water column NPP inventory as simulated by the
407 model, and spatially the offline calculated NPP is larger than the model output in oligotrophic
408 regions and smaller than the model output in coastal and upwelling regions as expected (not
409 shown). In addition, the temporal rate of change is somewhat smaller for the offline calculated
410 NPP (not shown). Note that the following results and discussion concerns only the offline
411 NPP calculations and therefore only the top 100 m of the ocean. The offline calculation shows
412 that in the top 100 m only CCT significantly changes NPP_{total} compared to RCP8.5. In fact,
413 CCT results in an increased productivity by 2100 (Figure 7a) in the offline calculation, which
414 is linked to the increase in the incoming solar radiation in some regions, since the shortwave
415 reflection from ice clouds is reduced. After termination of CCT, the NPP_{total} drops to the same
416 level as RCP8.5 within two years. The RCP4.5 scenario yields little change by 2100.

417 Warmer temperatures increase growth rates. Thus when only temperature is allowed to
418 change, NPP_{temp} increases in the offline calculation (Figure 7b), as temperature increases in
419 all scenarios considered here (Figure 1b), even though less in simulations with RM than
420 RCP8.5. All methods of RM yield an increase in NPP_{temp} of ~1% from 2020 to 2100,
421 comparable to RCP4.5. This is consistent with SST being comparable between RCP4.5 and
422 RM (Figure 1b). After termination, NPP_{temp} increases rapidly for the first five years, before
423 stabilizing with the same rate of change as that in RCP8.5. Just like SST (Figure 1b), the

424 absolute change in NPP_{temp} does not quite recover to the same absolute level as that in
425 RCP8.5, but all simulations show an increase in NPP_{temp} of ~3% by 2150.

426 Reduced shortwave radiation at the surface decreases growth rates and thus lead to
427 decreased NPP. In RCP4.5 and RCP8.5, light constraints do not change much, hence when
428 using the output from these experiments and only shortwave radiation changes in the offline
429 calculation, NPP_{light} does not considerably change (Figure 7c). Both SAI and MSB decrease
430 the amount of global mean direct shortwave radiation at the surface, however, which
431 negatively affect the phytoplankton growth rate and NPP_{light} in the ocean (Figure 7c). The
432 result is therefore a decrease in NPP_{light} of ~2% by 2100 for SAI and MSB (Figure 7c). When
433 reducing the optical thickness and the lifetime of the cirrus clouds in the model, the shortwave
434 reflection by these clouds is reduced, allowing more shortwave radiation to reach the surface
435 and increasing the growth rate. CCT thus results in an increase in NPP_{light} of ~2% by 2100
436 (Figure 7c). It is this increase in available shortwave radiation that causes the majority of the
437 increase in ocean productivity with CCT, with some contribution from the elevated
438 temperatures (Figure 7b). Within two years of the termination of RM, the NPP_{light} has
439 completely returned to the baseline conditions.

440 There cannot be any growth of phytoplankton without nutrients. However, changes in
441 the concentration of the limiting nutrient (either phosphate, nitrate, or dissolved iron) has a
442 small effect on the growth rate (not shown). NPP is the product of growth rate and
443 phytoplankton concentration (Equation 2), but phytoplankton concentration is also a function
444 of growth rate, as well as grazing, aggregation, and mortality. In the model, the time step is
445 small and the relationships are fully dynamic within the NPZD framework. However, since
446 we use monthly model output in the offline calculation, the phytoplankton concentration is
447 not independent of either the nutrient availability or the growth rate. Therefore we look at the
448 residual $NPP_{residual}$ ($NPP_{total} - NPP_{temp} - NPP_{light}$). This residual approximates the integrated

449 circulation-induced changes in phytoplankton concentration and the concentration of the
450 limiting nutrient. The latter is an important limiting factor for NPP, especially in the low
451 latitude regions, and is largely influenced by circulation changes. Figure 7d shows that
452 NPP_{residual} dominates over the growth rate in determining changes in ocean NPP. Overall,
453 NPP_{residual} accounts for a decrease of ~8% by 2100 in RCP8.5. The SAI and MSB methods of
454 RM also exhibit a change in NPP_{residual} , but the change of ~5% is less than that in RCP8.5.
455 With CCT there is no significant change in NPP_{residual} by 2100 relative to 1971-2000. After
456 termination, NPP_{residual} decreases rapidly and after 4-5 years it continues changing at a rate
457 comparable to that in RCP8.5, reaching a global mean reduction of greater than -10% in 2150.

458

459 **3.5 Regional changes in ocean NPP**

460 As seen in Figure 6, the projected changes in ocean NPP exhibit large spatial variation.
461 These spatial patterns are comparable to the NPP calculated offline (Figure 8). Applying RM
462 does not change the large-scale spatial heterogeneity, but rather works to enhance or weaken
463 the change magnitude (Figures 6 and 8). These regional differences are important, since
464 regional changes are much more important than global changes when determining the impact
465 ocean NPP has on human food security (Mora et al., 2013). For a more detailed analysis, five
466 regions have been identified and analyzed using the offline calculations of NPP and its
467 drivers. These regions are chosen based on:

- 468 (i) a significant change, i.e. outside of ± 1 standard deviation, in NPP in RCP8.5 in years
469 2071-2100 relative to 1971-2000;
- 470 (ii) the sign of the change in ocean NPP projected by NorESM1-ME being consistent
471 with that of the CMIP5 models ensemble mean (Bopp et al., 2013; Mora et al., 2013);

- 472 (iii) the impact the different methods of RM has on this increase or decrease in the online
473 simulations; and
474 (iv) their relative importance for fish catches, as identified in Zeller et al. (2016).

475 The regions are outlined in black in Figure 6b, and labeled the Equatorial Pacific,
476 Equatorial Atlantic, Southern Atlantic, Indian Ocean, and Sea of Okhotsk in Figure 9. In
477 RCP8.5, the Sea of Okhotsk and Southern Atlantic exhibit a significant increase in NPP in
478 2071-2100 relatively to 1971-2000, while the Equatorial Pacific, Indian Ocean, and
479 Equatorial Atlantic show a significant weakening (Figure 9).

480 The IPCC's Assessment Report 5 (AR5) states that, due to lack of consistent
481 observations, it remains uncertain how the future changes in marine ecosystem drivers (like
482 productivity, acidification, and oxygen concentrations) will alter the higher trophic levels
483 (Pörtner et al., 2014). Given the lack of complexity and lack of higher trophic level organisms
484 in the NorESM1-ME, we are unable to directly link changes in NPP to impacts on the higher
485 trophic levels in this study. It therefore cannot be assumed from our results that increased NPP
486 will lead to increased fish stocks and thus potential for higher fish catches, because the
487 driving factors leading to higher NPP (*i.e.* temperature, light availability, and stratification)
488 could also lead to biodiversity changes. Given the changes in Arctic biodiversity observed
489 today due to temperature changes (*e.g.* Bucholz et al., 2012; Fossheim et al., 2015), respective
490 changes in migration pattern would be likely to happen also with RM. Nevertheless, higher
491 NPP does lead to more food for higher trophic level organisms; therefore a significant
492 decrease in regional NPP could decrease higher trophic organisms due to less food availability
493 in those regions. Based on the model projections, it is possible that there will be less fish
494 catches in the Indian Ocean and Equatorial Atlantic in the future than today. The different
495 methods of RM also lead to different effects on ocean NPP (Figures 6 and 9). Only in the

496 Equatorial Atlantic, and in the shaded regions where there are no significant changes, do all
497 three methods give changes in NPP comparable to those in RCP4.5.

498 In the Equatorial Pacific, RCP8.5 leads to a decrease in ocean NPP of -21% in 2071-
499 2100 relative to 1971-2000, driven by circulation - induced changes in phytoplankton
500 concentration and nutrient availability. Circulation - induced changes dominates the change of
501 -12% in RCP4.5 too. This region is today a very productive fishery area (Zeller et al., 2016),
502 so a significant decrease in NPP could have adverse effects on fish catches. It is therefore
503 noteworthy that all RM methods yield NPP changes only marginally smaller than those in
504 RCP8.5, and not nearly as small as those in RCP4.5. When RM is applied, shortwave
505 radiation changes at the surface become more important in driving NPP changes than they are
506 in RCP8.5 and RCP4.5, which is consistent with changes in cloud fraction (not shown, see
507 Muri et al., 2017). With CCT, the radiation changes yield an increase in NPP of 5%,
508 indicating that this is one of the regions that drive the global mean increase in NPP (Figure
509 7a). After termination, the change in NPP is comparable to that in RCP8.5 in all experiments,
510 and the warming results in a small increase in NPP of ~2% (Figure 7b).

511 The Southern Atlantic has the largest changes in 2071-2100 relative to 1971-2000,
512 where RCP8.5 results in an increase in ocean NPP of 39% and RCP4.5 leads to an increase of
513 25%. SAI leads to changes in NPP comparable to that in RCP8.5, while MSB and CCT yield
514 changes more in line with RCP4.5. For all experiments, the circulation-induced changes are
515 the dominant factor. Changes in temperatures contribute ~5% to the total change, which is
516 consistent with a significant warming in all experiments (Figure 3). This alleviates the
517 temperature limitation of the growth rate, which is consistent with the other CMIP5 models
518 (Bopp et al., 2013). After termination, the increase continues in the Southern Atlantic, and in
519 2121-2150 the changes in NPP are 60-70% higher than in 1971-2000 in all experiments.

520 As in all other regions, in the Sea of Okhotsk, the circulation-induced changes
521 dominate. SAI and MSB both yield changes comparable to that in RCP4.5, while CCT, on the
522 other hand, is comparable to RCP8.5. In all experiments, temperature changes are an
523 important driver of the overall increases in NPP, consistent with the strong warming in this
524 region (Figure 3). After termination, all experiments yield comparable increases in NPP, with
525 a very strong contribution from the temperature changes.

526 In the Equatorial Atlantic, there is a reduction of ocean NPP in RCP8.5 of -19% in
527 2071-2100 relative to 1971-2000. Circulation-induced changes dominate this change, with a
528 minor negative contribution of <5% from radiation changes. All methods of RM yield
529 changes in ocean NPP more in line with that in RCP4.5 (-11%), but changes in radiation are
530 more important with SAI and MSB. After termination, all experiments result in the same
531 decrease in ocean NPP of -25%.

532 In the Indian Ocean, there is also a reduction of ocean NPP in RCP8.5. Here the total
533 change in 2071-2100 is -21%, but unlike in any other regions the temperature-induced
534 changes lead to only a small increase of 1-2% in all experiments. This is consistent with parts
535 of this region experiencing only a small increase in SST (Figure 3). Both SAI and MSB yield
536 changes in NPP comparable to that in RCP8.5 (-19% and -18% respectively), but where
537 changes in radiation contribute ~-2% to the total reduction. There is, however, no
538 corresponding change in cloud cover (see Muri et al., 2017) to explain the apparent
539 importance of radiation changes in this region. The Indian Ocean is also one of the regions
540 where CCT is able to sustain (i.e., induce least changes in) the contemporary NPP. After
541 termination, the ocean NPP continues to decrease and is in 2121-2150 30% lower than in
542 1971-2000 in all experiments.

543

544 **3.6 Comparison with previous studies**

545 Very few other studies have been published on the impact on ocean biogeochemistry
546 due to RM. One such study is by Hardman-Mountford et al. (2013), which used a one-
547 dimensional water column model to study the effect of reduced light availability on
548 phytoplankton growth. Their results imply that even a significant reduction (90%) of solar
549 radiation barely affects total column biological productivity, but can alter considerably
550 vertical distribution of productivity. However, their study did not consider how other
551 processes, such as local cooling or horizontal transport of nutrients, would affect the marine
552 ecosystems, and their simplistic model setup was also unable to capture broader effects on the
553 ocean carbon cycle. The magnitude of regional changes in NPP found in this study differs
554 from the results of Hardman-Mountford et al. (2013), but the NPP changes seen in the
555 oligotrophic gyres are very small and not statistically significant. Given the very large
556 differences in method, no in depth comparison of this study and Hardman-Mountford et al.
557 (2013) has been undertaken. Two other recent studies, which are both more comparable to
558 this one, are Tjiputra et al. (2016) and Partanen et al. (2016). Tjiputra et al. (2016), who used
559 the same model as in this study, identified changes in ocean NPP and export production in a
560 simulation with SAI. The implementation of SAI is different here, both in methodology
561 somewhat and magnitude of forcing, but the spatial pattern and sign of surface climate
562 response and the overall impact on global ocean NPP are broadly consistent. Nevertheless,
563 our study provides a more extended and in-depth analysis based on different RM methods as
564 well as identifies dominant drivers of changes in NPP in key ocean regions. Partanen et al.
565 (2016), on the other hand, analyzed the effects on ocean NPP from marine cloud brightening
566 (MCB) only. Overall, the effects in this study and that of Partanen et al. (2016) are quite
567 different. Spatially, Partanen et al. (2016) sees a very strong correlation between the regions
568 where the cloud brightening forcing was applied and the regions of strongest NPP change,

569 which is not apparent in this study. Temporally, the change in NPP in Partanen et al. (2016)
570 comes in form of a relatively rapid decrease over the first ten years, when the cloud
571 brightening forcing is applied, while in this study the change is more even throughout the
572 period of MSB forcing. This is likely due to the several noteworthy differences between their
573 method and the one used here:

- 574 (i) Partanen et al. (2016) uses the UVic ESCM model, an Earth system model of
575 intermediate complexity (EMIC), while here we use the fully coupled NorESM1-ME
576 Earth system model;
- 577 (ii) Here, we increase oceanic sea salt emissions over $\pm 45^\circ$ latitude not only brightening
578 the marine stratocumulus decks, but also reflecting more shortwave radiation with the
579 increased in bright aerosols through the direct effect. Partanen et al. (2016), on the
580 other hand, prescribe changes in radiation over three marine stratocumulus areas
581 inferred from model output from Partanen et al. (2012).
- 582 (iii) The RM forcing applied by Partanen et al. (2016) is -1 Wm^{-2} annually, while here it is
583 ramped up to -4 Wm^{-2} in 2100;
- 584 (iv) Partanen et al. (2016) applies RM to RCP4.5, while here we apply RM to RCP8.5;
- 585 (v) Partanen et al. (2016) applies RM for 20 years before termination, while here we
586 apply RM for 80 year before termination, which, combined with the higher forcing,
587 means that the Earth system takes longer to recover in this study than in the Partanen
588 et al. (2016) study.

589 The biggest and most important of these differences is that Partanen et al. (2016) use
590 an EMIC, while we use an ESM with the forcing applied over a much larger area. NorESM1-
591 ME has a fully interactive tropospheric aerosol scheme, accounting for both the direct and the
592 indirect effects of the aerosols, which is of key importance when evaluating the impact of
593 changes in shortwave radiation reaching the surface from changes to clouds. Partanen et al.

594 (2016) take their forcing from Partanen et al. (2012), which use an atmosphere-only version
595 of their model and hence neglect important feedbacks, including SST and ocean feedbacks.
596 Partanen et al. (2016) furthermore prescribe their forcing in terms of changes to the radiation,
597 and hence miss out on further feedbacks with their one layered atmosphere with prescribed
598 circulation, processes that are much more comprehensively represented in our fully coupled
599 Earth system model. MSB may, *e.g.*, lead to an increased sinking of air over the oceans and
600 hence a reduction in cloud cover, as seen in both Ahlm et al. (2017), Stjern et al. (2017) and
601 Muri et al. (2017). The ecosystem module in NorESM1-ME is not substantially more
602 complex than that of the UViC ESCM model, but differences could arise due to better
603 representation of the ocean physical circulation (owing to higher spatial resolution) and air-
604 sea interactions. Partanen et al. (2016) identify a decrease in global mean ocean NPP relative
605 to their reference case (RCP4.5), while in our MSB simulation we simulate an increase in
606 ocean NPP relative to our reference case (RCP8.5). This likely impacts the differences in
607 results since the global mean and rate of change of ecosystem drivers in RCP4.5 are smaller
608 than RCP8.5 (Henson et al., 2017). These methodological differences and the large
609 differences in the spatial impact can partly be explained by the differences in the applied RM
610 forcing and method, but is mostly explained by the fundamental differences between the
611 models. Another important difference between Partanen et al. (2016) and this study, is the
612 timing of termination, since this is a very important aspect of all climate engineering studies.
613 Partanen et al. (2016) applies RM for 20 years before termination, while we apply RM for 80
614 years before termination. This means that in our study the impact on temperature and ocean
615 circulation is greater than in the Partanen et al. (2016) study, as the slow climate feedbacks
616 are allowed to pan out. This could explain the differences in termination effect between the
617 studies, where the NPP fully recovers and exceeds that in RCP4.5 in the Partanen et al. (2016)
618 study, but remain within the variability of RCP8.5 here. The larger magnitude of the forcing

619 applied in our simulations (-4 Wm^{-2} in 2100) also means that it takes much longer for the
620 climate system to recover back to the RCP8.5 state.

621

622 **4 CONCLUSIONS**

623 In this study, we use the Norwegian Earth System Model with fully interactive carbon
624 cycle to assess the impact of three radiation management climate engineering (RM) methods
625 on marine biogeochemistry. The model simulations indicate that RM may reduce
626 perturbations in SST and thermocline oxygen driven by anthropogenic climate change, but
627 that large changes in NPP remain and are even intensified in some regions. It must be noted,
628 that we use only one model, and that such models are known to have large spread in their
629 projections of future ocean NPP (*e.g.* Bopp et al., 2013). However, this single-model study
630 does show some clear tendencies:

- 631 (i) A clear mitigation of the global mean decrease in ocean NPP from 10% in 2100 in
632 RCP8.5 and ~5% in RCP4.5 to somewhere between 3% and 6%, depending on the
633 method of RM.
- 634 (ii) Strong regional variations in the changes, and what primarily drives the changes, in
635 ocean NPP. The different methods of RM do not have the same effects in the same
636 regions, even though SAI and MSB yield similar global averages.
- 637 (iii) Spatially MSB yields the largest changes relative to RCP4.5, which is consistent with
638 MSB being applied over the ocean and therefore likely affects the ocean more
639 strongly than the other methods.

640 The effect of future climate change on ocean NPP is uncertain, and is driven by an
641 integrated change in physical factors, such as temperature, radiation, and ocean mixing.
642 Additionally, changes in ocean oxygen concentrations and ocean acidification are likely to

643 affect ocean NPP. It is noteworthy that with RM, the way the scenario is designed in this
644 study, anthropogenic CO₂ emissions are not curbed, so ocean acidification would continue.
645 The results presented in this study show that future changes to ocean NPP would likely be
646 negative on average, but exhibit great variation both temporally and spatially, regardless of
647 whether or not RM is applied.

648 This study also show that for the first five to ten years after a sudden termination of
649 large-scale RM with no mitigation or CDR efforts, the SST, oxygen, surface pH, and NPP all
650 experience changes that are significantly larger than those projected without RM
651 implementation or mitigation. While there is still large uncertainty in how marine habitats
652 respond to such rapid changes, it is certain than they will have less time to adapt or migrate to
653 a more suitable location and potentially have higher likelihood to face extinction, if RM was
654 suddenly halted during large-scale deployment and with no mitigation.

655 The results of this work does nothing to diminish the complexity of climate impacts on
656 NPP, but rather highlights that any change in ocean NPP is driven by a combination of several
657 variables, which all change in different ways in the future, and subsequently are affected
658 differently when RM is applied. The importance of ocean NPP for human societies, however,
659 lies in its impact on food security in general and fisheries in particular, for which regional
660 changes are much more important than global changes (Mora et al., 2013).

661

662 **ACKNOWLEDGEMENTS**

663 The authors acknowledge funding from the Norwegian Research Council through the project
664 EXPECT (229760). We also acknowledge NOTUR resource NN9182K, Norstore NS9033K
665 and NS1002K. Helene Muri was also supported by RCN project 261862/E10, 1.5C-BECCSy.
666 JT also acknowledges RCN project ORGANIC (239965). The authors want to thank Alf Grini

667 for his technical assistance in setting up and running model experiments, as well as the rest of
668 the EXPECT team

669

670 REFERENCES

- 671 Ahlm, L., Jones, A., Stjern, C. W., Muri, H., Kravitz, B., and Kristjánsson, J. E.: Marine
672 cloud brightening – as effective without clouds, *Atmos. Chem. Phys. Discuss.*, 2017, 1-
673 25, 2017. doi:10.5194/acp-2017-484.
- 674 Alterskjær, K., Kristjánsson, J. E., Boucher, O., Muri, H., Niemeier, U., Schmidt, H., Schulz,
675 M., and Timmreck, C.: Sea-salt injections into the low-latitude marine boundary layer:
676 The transient response in three Earth system models, *J. Geophys. Res.-Atmos.*, 118,
677 12195-12206, 2013. doi:10.1002/2013jd020432.
- 678 Aswathy, N., Boucher, O., Quaas, M., Niemeier, U., Muri, H., Mulmenstadt, J., and Quaas, J.:
679 Climate extremes in multi-model simulations of stratospheric aerosol and marine cloud
680 brightening climate engineering, *Atmospheric Chemistry and Physics*, 15, 9593-9610,
681 2015. doi:10.5194/acp-15-9593-2015
- 682 Bala, G., Caldeira, K., Nemani, R., Cao, L., Ban-Weiss, G., and Shin, H.-J. Albedo
683 enhancement of marine clouds to counteract global warming: impacts on the hydrological
684 cycle. *Climate Dynamics* 37(5-6), 915–931, 2011. doi: 10.1007/s00382-010-0868-1.
- 685 Bentsen, M., Bethke, I., Debernard, J. B., Iversen, T., Kirkevåg, A., Seland, Ø., Drange, H.,
686 Roelandt, C., Seierstad, I. A., Hoose, C., and Kristjánsson, J. E.: The Norwegian Earth
687 System Model, NorESM1-M – Part 1: Description and basic evaluation of the physical
688 climate, *Geosci. Model Dev.*, 6, 687-720, 2013. doi:10.5194/gmd-6-687-2013
- 689 Bickel J, and Lane L. *An Analysis of Climate Engineering as a Response to Climate Change.*
690 Frederiksberg: Copenhagen Consensus Center. 2009.
- 691 Bopp, L., Resplandy, L., Orr, J. C., Doney, S. C., Dunne, J. P., Gehlen, M., Halloran, P.,
692 Heinze, C., Ilyina, T., Seferian, R., Tjiputra, J., and Vichi, M.: Multiple stressors of ocean
693 ecosystems in the 21st century: projections with CMIP5 models, *Biogeosciences*, 10,
694 6225-6245, 2013. doi:10.5194/bg-10-6225-2013
- 695 Buchholz, F., Werner, T., and Buchholz, C.: First observation of krill spawning in the high
696 Arctic Kongsfjorden, west Spitsbergen, *Polar Biology*, 35, 1273-1279, 2012.
697 doi:10.1007/s00300-012-1186-3
- 698 Crook, J. A., Jackson, L. S., Osprey, S. M., and Forster, P. M.: A comparison of temperature
699 and precipitation responses to different Earth radiation management geoengineering
700 schemes, *J. Geophys. Res.-Atmos.*, 120, 9352-9373, 2015. doi:10.1002/2015jd023269
- 701 Crutzen, P. J.: Albedo enhancement by stratospheric sulfur injections: A contribution to
702 resolve a policy dilemma? *Climatic Change*, 77, 211-219, 2006. doi:10.1007/s10584-006-
703 9101-y
- 704 Fossheim, M., Primicerio, R., Johannesen, E., Ingvaldsen, R. B., Aschan, M. M., and Dolgov,
705 A. V.: Recent warming leads to a rapid borealization of fish communities in the Arctic,
706 *Nat. Clim. Chang.*, 5, 673-677, 2015. doi:10.1038/nclimate2647
- 707 Friedlingstein, P., Cox, P., Betts, R., Bopp, L., von Bloh, W., Brovkin, V., Cadule, P., Doney,
708 S., Eby, M., Fung, I., Bala, G., John, J., Jones, C., Joos, F., Kato, T., Kawamiya, M.,
709 Knorr, W., Kindsay, K., Matthews, H. D., Raddatz, T., Rayner, P., Reick, C., Roeckner,
710 E., Schnitzler, K.-G., Schnur, R., Strassmann, K., Weaver, A. J., Yoshikawa, C., and

711 Zeng, N.: Climate-Carbon Cycle Feedback Analysis: Results from the C4MIP Model
712 Intercomparison, *Journal of Climate*, 19, 3337-3353, 2006.

713 Henson, S. A., Beaulieu, C., Ilyina, T., John, J. G., Long, M., Séférian, R., Tjiputra, J., and
714 Sarmiento, J. L.: Rapid emergence of climate change in environmental drivers of marine
715 ecosystems, *Nat. Commun.*, 8, 14682, 2017. doi:10.1038/ncomms14682

716 Hardman-Mountford, N. J., Polimene, L., Hirata, T., Brewin, R. J. W., and Aiken, J.: Impacts
717 of light shading and nutrient enrichment geo-engineering approaches on the productivity
718 of a stratified, oligotrophic ocean ecosystem, *J. R. Soc. Interface*, 10, 9, 2013.
719 doi:10.1098/rsif.2013.0701

720 IPCC, 2013: Climate Change 2013: The Physical Science Basis. Contribution of Working
721 Group I to the Fifth Assessment Report of the Intergovernmental Panel on Climate
722 Change [Stocker, T.F., D. Qin, G.-K. Plattner, M. Tignor, S.K. Allen, J. Boschung, A.
723 Nauels, Y. Xia, V. Bex and P.M. Midgley (eds.)]. Cambridge University Press,
724 Cambridge, United Kingdom and New York, NY, USA, 1535 pp.

725 Irvine, P. J., Kravitz, B., Lawrence, M. G., and Muri, H.: An overview of the Earth system
726 science of solar geoengineering. *WIREs Climate Change* 7: 815–833, 2016. doi:
727 10.1002/wcc.423.

728 Irvine, P. J., Kravitz, B., Lawrence, M. G., Gerten, D., Caminade, C., Gosling, S. N., Hendy,
729 E., Kassie, B., Kissling, W. D., Muri, H., Oschlies, A., and Smith, S. J.: Towards a
730 comprehensive climate impacts assessment of solar geoengineering, *Earth's Future*, 2016.
731 doi:10.1002/2016EF000389.

732 Kristjansson, J. E., Muri, H., and Schmidt, H.: The hydrological cycle response to cirrus cloud
733 thinning, *Geophysical Research Letters*, 42, 10807-10815, 2015.
734 doi:10.1002/2015gl066795

735 Latham, J.: Control of Global Warming, *Nature*, 347, 339-340, 1990. doi:10.1038/347339b0

736 Lynch, D. K.: *Cirrus*, Oxford University Press, 2002.

737 Ma, X., von Salzen, K., and Li, J.: Modelling sea salt aerosol and its direct and indirect effects
738 on climate, *Atmospheric Chemistry and Physics*, 8, 1311-1327, 2008.

739 Maier-Reimer, E., Kriest, I., Segschneider, J., and Wetzol, P.: The Hamburg Oceanic Carbon
740 Cycle Circulation model HAMOCC5.1, Max Planck Institute for Meteorology, Hamburg,
741 Germany, 2005.

742 Matthews, H. D., Cao, L., and Caldeira, K.: Sensitivity of ocean acidification to
743 geoengineered climate stabilization, *Geophysical Research Letters*, 36, 2009.
744 doi:10.1029/2009gl037488

745 Mitchell, D., L. and Finnegan, W.: Modification of cirrus clouds to reduce global warming,
746 *Environmental Research Letters*, 4, 045102, 2009. doi:10.1088/1748-9326/4/4/045102

747 Muri, H., Kristjansson, J. E., Storelvmo, T., and Pfeffer, M. A.: The climatic effects of
748 modifying cirrus clouds in a climate engineering framework, *J. Geophys. Res.-Atmos.*,
749 119, 4174-4191, 2014. doi:10.1002/2013jd021063

750 Muri, H., Tjiputra, J., Otterå, O. H., Adakudlu, M., Lauvset, S. K., Grini, A., Schulz, M., and
751 Kristjansson, J. E.: Climate response to aerosol injection geoengineering: a multi-method
752 comparison. *Journal of eClimate* (under review), 2017. doi: 10.1175/JCLI-D-17-0620.1.

753 Niemeier, U., Schmidt, H., Alterskjaer, K., and Kristjansson, J. E.: Solar irradiance reduction
754 via climate engineering: Impact of different techniques on the energy balance and the
755 hydrological cycle, *J. Geophys. Res.-Atmos.*, 118, 11905-11917, 2013.
756 doi:10.1002/2013jd020445.

757 Niemeier, U. and Timmreck, C.: What is the limit of climate engineering by stratospheric
758 injection of SO₂?, *Atmos. Chem. Phys.*, 15, 9129-9141, [https://doi.org/10.5194/acp-15-](https://doi.org/10.5194/acp-15-9129-2015)
759 9129-2015, 2015.

760 Partanen, A.-I., Kokkola, H., Romakkaniemi, S., Kerminen, V. M., Lehtinen, K. E. J.,
761 Bergman, T., Arola, A., and Korhonen, H.: Direct and indirect effects of sea spray
762 geoengineering and the role of injected particle size, *J. Geophys. Res.*, 117, D02203,
763 2012. doi:10.1029/2011JD016428.

764 Partanen, A.-I., Keller, D. P., Korhonen, H., and Matthews, H. D.: Impacts of sea spray
765 geoengineering on ocean biogeochemistry, *Geophysical Research Letters*, 43, 7600-7608,
766 2016. doi:10.1002/2016gl070111

767 Pörtner, H.-O., Karl, D. M., Boyd, P. W., Cheung, W. W. L., Lluich-Cota, S. E., Nojiri, Y.,
768 Schmidt, D. N., and Zavialov, P. O.: Ocean systems. In: *Climate Change 2014: Impacts,*
769 *Adaptation, and Vulnerability. Part A: Global and Sectoral Aspects. Contribution of*
770 *Working Group II to the Fifth Assessment Report of the Intergovernmental Panel on*
771 *Climate Change*, edited by C. B. Field et al., pp. 411– 484, Cambridge University Press,
772 Cambridge, United Kingdom and New York, NY, USA. 2014

773 Riahi, K., Rao, S., Krey, V., Cho, C. H., Chirkov, V., Fischer, G., Kindermann, G.,
774 Nakicenovic, N., and Rafaj, P.: RCP 8.5-A scenario of comparatively high greenhouse
775 gas emissions, *Climatic Change*, 109, 33-57, 2011. doi:10.1007/s10584-011-0149-y

776 Six, K. D. and Maier-Reimer, E.: Effects of plankton dynamics on seasonal carbon fluxes in
777 an ocean general circulation model, *Global Biogeochemical Cycles*, 10, 559-583, 1996.
778 doi:10.1029/96gb02561

779 Stjern, C. W., Muri, H., Ahlm, L., Boucher, O., Cole, J. N. S., Ji, D., Jones, A., Haywood, J.
780 M., Kravitz, B., Lenton, A., Moore, J. C., Niemeier, U., Phipps, S. J., Schmidt, H.,
781 Watanabe, S., and Kristjánsson, J. E.: Response to marine cloud brightening in a multi-
782 model ensemble. *Atmospheric Chemistry and Physics Discussions*. 2017. doi:
783 10.5194/acp-2017-629.

784 Storelvmo, T., Kristjánsson, J. E., Muri, H., Pfeffer, M., Barahona, D., and Nenes, A.: Cirrus
785 cloud seeding has potential to cool climate, *Geophysical Research Letters*, 40, 178-182,
786 2013. doi:10.1029/2012gl054201

787 Teller, E., Hyde, R., Ishikawa M., et al. *Active Stabilization of Climate: Inexpensive,*
788 *Lowrisk, near-Term Options for Preventing Global Warming and Ice Ages Via*
789 *Technologically Varied Solar Radiative Forcing*. Lawrence Livermore National Library,
790 30 November. 2003

791 Thomson, A. M., Calvin, K. V., Smith, S. J., Kyle, G. P., Volke, A., Patel, P., Delgado-Arias,
792 S., Bond-Lamberty, B., Wise, M. A., Clarke, L. E., and Edmonds, J. A.: RCP4.5: a
793 pathway for stabilization of radiative forcing by 2100, *Climatic Change*, 109, 77-94,
794 2011. doi:10.1007/s10584-011-0151-4

795 Tjiputra, J. F., Grini, A., and Lee, H.: Impact of idealized future stratospheric aerosol
796 injection on the large scale ocean and land carbon cycles, *Journal of Geophysical*
797 *Research: Biogeosciences*, 120, doi: 10.1002/2015jg003045, 2016.
798 doi:10.1002/2015jg003045

799 Tjiputra, J. F., Roelandt, C., Bentsen, M., Lawrence, D. M., Lorentzen, T., Schwinger, J.,
800 Seland, O., and Heinze, C.: Evaluation of the carbon cycle components in the Norwegian
801 Earth System Model (NorESM), *Geoscientific Model Development*, 6, 301-325, 2013.
802 doi:10.5194/gmd-6-301-2013

803 Wanninkhof, R.: Relationship between wind speed and gas exchange over the ocean, *Journal*
804 *of Geophysical Research*, 97, 7373-7382, 1992.

805 Weisenstein, D. K., Keith, D. W., and Dykema, J. A.: Solar geoengineering using solid
806 aerosol in the stratosphere, *Atmospheric Chemistry and Physics*, 15, 11835-11859, 2015.
807 doi:10.5194/acp-15-11835-2015

808 Wigley, T.M.L., A combined mitigation/geoengineering approach to climate stabilization,
809 *Science* 314:452-454. 2006. doi:10.1126/science.1131728

810 Xia, L., Robock, A., Tilmes, S., and Neely Iii, R. R.: Stratospheric sulfate geoengineering
811 could enhance the terrestrial photosynthesis rate, *Atmospheric Chemistry and Physics*,
812 16, 1479-1489, 2016. doi:10.5194/acp-16-1479-2016
813 Zeller, D., Palomares, M. L. D., Tavakolie, A., Ang, M., Belhabib, D., Cheung, W. W. L.,
814 Lam, V. W. Y., Sy, E., Tsui, G., Zyllich, K., and Pauly, D.: Still catching attention: Sea
815 Around Us reconstructed global catch data, their spatial expression and public
816 accessibility, *Marine Policy*, 70, 145-152, 2016. doi:10.1016/j.marpol.2016.04.046
817

818 FIGURES AND TABLES

819 **Figure 1.** Time series of global average change in (a) oxygen content at 200-600m depth (%), and (b) SST (°C).
820 The oxygen change is relative to the 1971-2000 average in the historical run.

821
822 **Figure 2.** The absolute change in oxygen concentration (200-600m) in 2071-2100 relative to 1971-2000 (in
823 moles O₂ m⁻²). Panel (a) shows zonally averaged (in 2° latitude bands) change for all simulations. Global maps
824 of (b) RCP8.5, (c) RCP4.5, (d) RCP8.5 with SAI, (e) RCP8.5 with MSB, (f) RCP8.5 with CCT. Gray shading in b)-f)
825 indicates areas where the change is not significantly different from the 1971-2000 average (*i.e.* within one
826 standard deviation of the 1971-2000 mean).

827
828 **Figure 3.** The absolute change in sea surface temperature (SST) in 2071-2100 relative to 1971-2000 (in °C).
829 Panel (a) shows zonally averaged (in 2° latitude bands) change for all simulations. Global maps of (b) RCP8.5,
830 (c) RCP4.5, (d) RCP8.5 with SAI, (e) RCP8.5 with MSB, (f) RCP8.5 with CCT. Gray shading in b)-f) indicates
831 areas where the change is not significantly different from the 1971-2000 average (*i.e.* within one standard
832 deviation of the 1971-2000 mean).

833
834 **Figure 4.** Time series of global average change in (a) atmospheric CO₂ (ppm), (b) air-sea CO₂ flux (PgC yr⁻¹), (c)
835 global surface ocean pH, (d) global deep ocean (>2000 m) pH, and (e) deep (>2000 m) North Atlantic Ocean
836 (north of 30°N) pH.

837
838 **Figure 5.** Time series of changes global ocean NPP (%). The NPP change is relative to the 1971-2000 average
839 in the historical run.

840
841 **Figure 6.** The percent changes in NPP in 2071-2100 relative to the 1971-2000 average in the historical run. (a)
842 Zonally averaged (in 2° latitude bands) change for all simulations. (b) RCP8.5, (c) RCP4.5, (d) RCP8.5 with SAI,
843 (e) RCP8.5 with MSB, (f) RCP8.5 with CCT. Gray shading in b)-f) indicates areas where the change is not
844 significantly different from the 1971-2000 average (*i.e.* within one standard deviation of the 1971-2000
845 mean). The outlined areas in panel (b) indicate regions plotted in Figure 10.

846
847 **Figure 7.** Time series of the 5-year running mean of globally averaged NPP (%) calculated offline using
848 Equations 1-3, plotted as the percent change relative to the 1971-2000 average in the historical run. The
849 residual ($NPP_{total} - NPP_{temp} - NPP_{light}$) represents the circulation-induced changes. Note the different scales on
850 the y-axes. See Table 1 for an explanation of the different calculations shown.

851
852 **Figure 8.** The percent change in the offline calculated NPP in 2071-2100 relative to the 1971-2000 average in
853 the historical run. (a) Zonally averaged (in 2° latitude bands) change for all simulations. (b) RCP8.5, (c)
854 RCP4.5, (d) RCP8.5 with SAI, (e) RCP8.5 with MSB, (f) RCP8.5 with CCT. Gray shading in b)-f) indicates areas
855 where the change is not significantly different from the 1971-2000 average (*i.e.* within one standard
856 deviation of the 1971-2000 mean). The outlined areas in panel (b) indicate regions plotted in Figure 9.

857
858 **Figure 9.** Offline calculated NPP change (%) in five different regions (as indicated on Figure 6b) for RCP4.5,
859 RCP8.5, and RCP8.5 with three different RM methods. The residual ($NPP_{total} - NPP_{temp} - NPP_{light}$) represents
860 the circulation-induced changes.

861
862
863
864
865
866
867
868
869
870
871
872
873
874

Table 1. Description of the offline calculations of ocean NPP and primary drivers using Equations 1-3. T is the average temperature in the top 100 m, L is shortwave radiation attenuated to 50 m depth, N is the concentration of the limiting nutrient (either nitrate, phosphate, or dissolved iron) in the top 100 m, and P is the concentration of phytoplankton cells in the top 100 m. \bar{X} denotes the long-term (80 year) mean of the given variable.

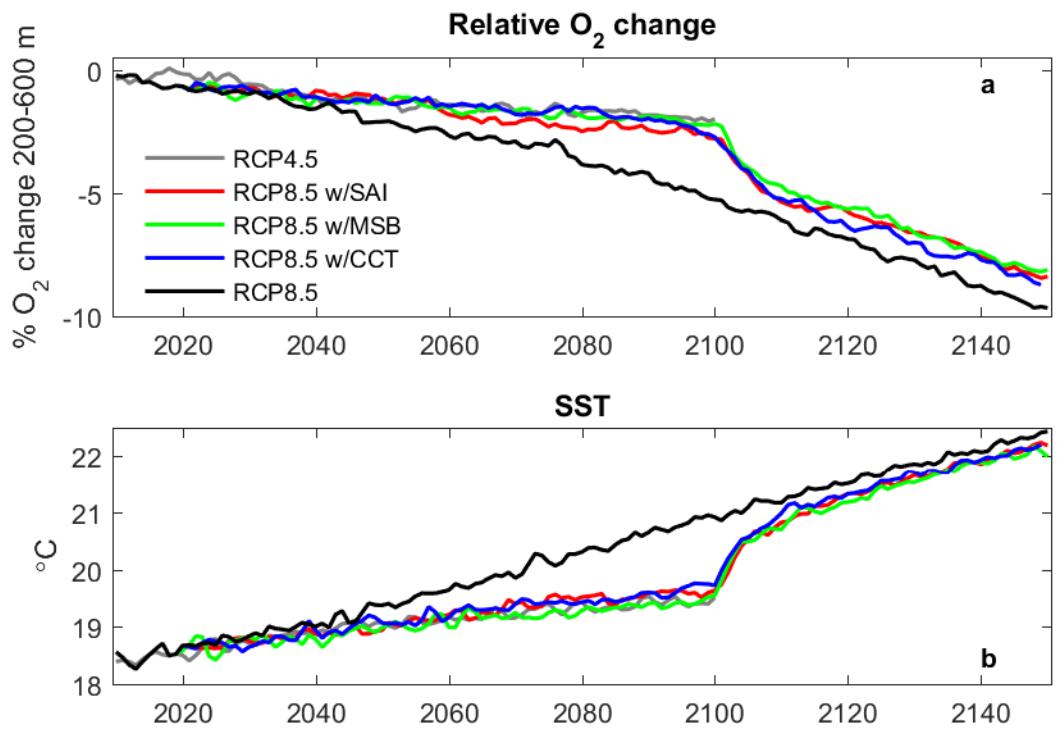
Calculation	
NPP _{total} Everything changes	T, L, N, P
NPP _{temp} Only temperature changes	T, \bar{L} , \bar{N} , \bar{P}
NPP _{light} Only shortwave radiation changes	L, \bar{T} , \bar{N} , \bar{P}
NPP _{residual}	NPP _{total} – NPP _{temp} – NPP _{light}

875

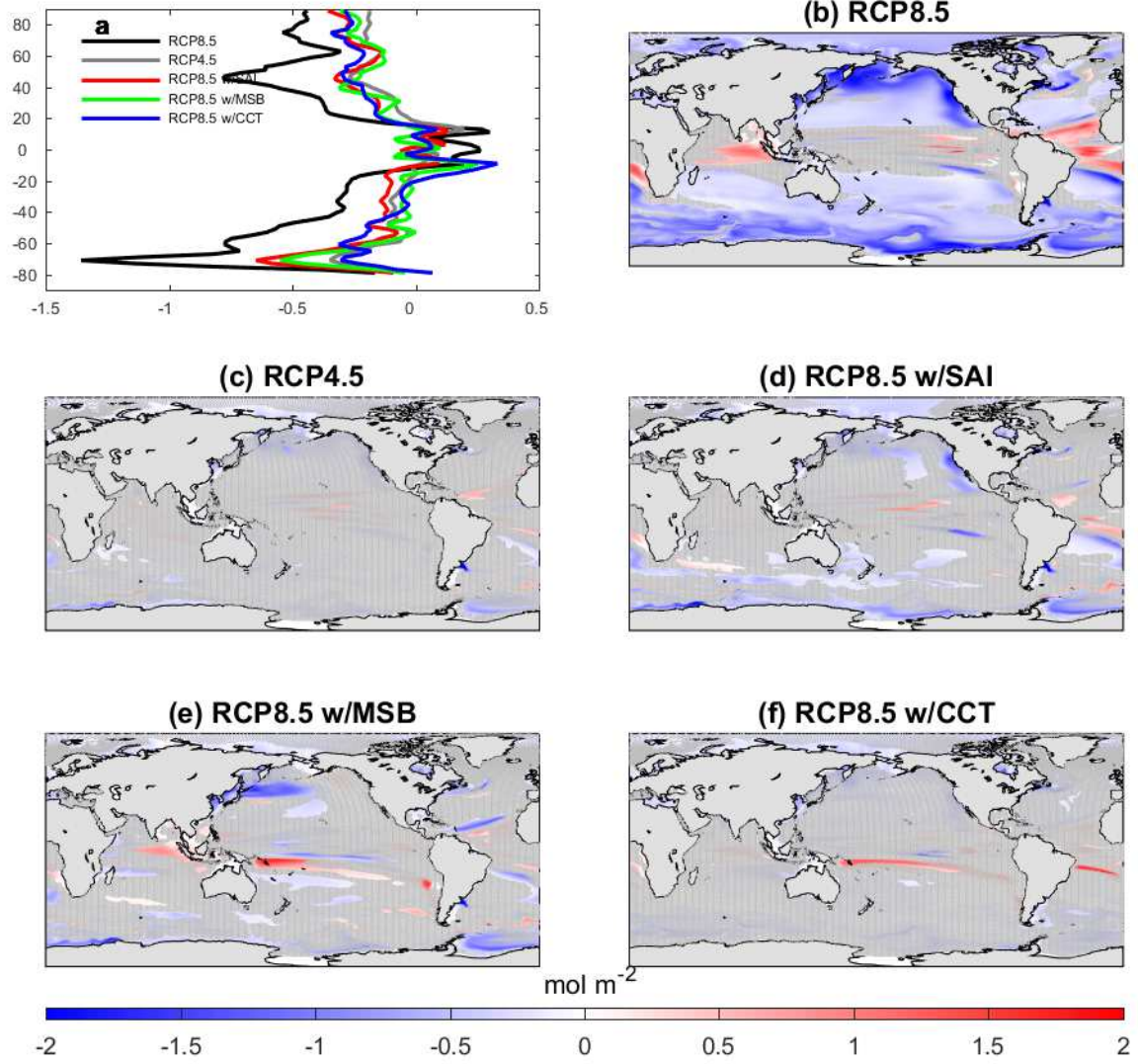
Table 2. General description of model experiments used in this study.

Experiment	Description	Time period
RCP4.5	Reference RCP4.5 scenario	2006-2100
RCP8.5	Reference RCP8.5 scenario	2006-2150
SAI	RCP8.5 scenario with a layer of sulfate particles is prescribed in the stratosphere to reflect incoming shortwave radiation and bring down global average temperatures	2020-2100
SAI _{EXT}	The extension of the SAI run after termination of climate engineering in 2100	2101-2150
MSB	RCP8.5 scenario where salt particles are emitted at the sea surface between 45°S and 45°N to make both the sky and clouds brighter, thus increasing the Earth's albedo thereby lower global average temperatures	2020-2100
MSB _{EXT}	The extension of the MSB run after termination of climate engineering in 2100	2101-2150
CCT	RCP8.5 scenario where cirrus clouds are thinned out. Cirrus clouds have a net heating effect so less ice clouds will result in lower global average temperatures	2020-2100
CCT _{EXT}	The extension of the CCT run after termination of climate engineering in 2100	2101-2150

877

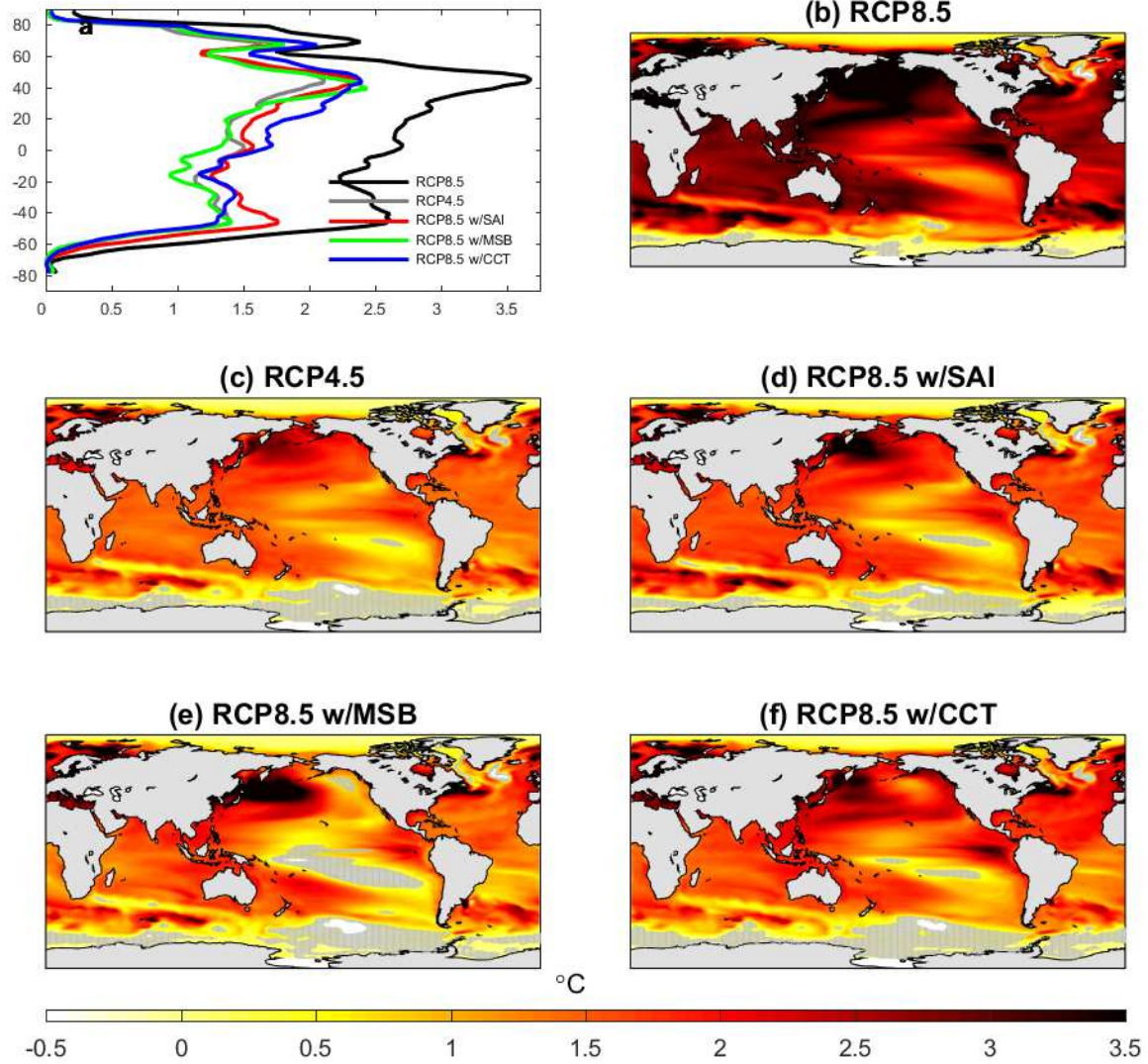


878 **Figure 1**



879 **Figure 2**

880



881 **Figure 3**

882

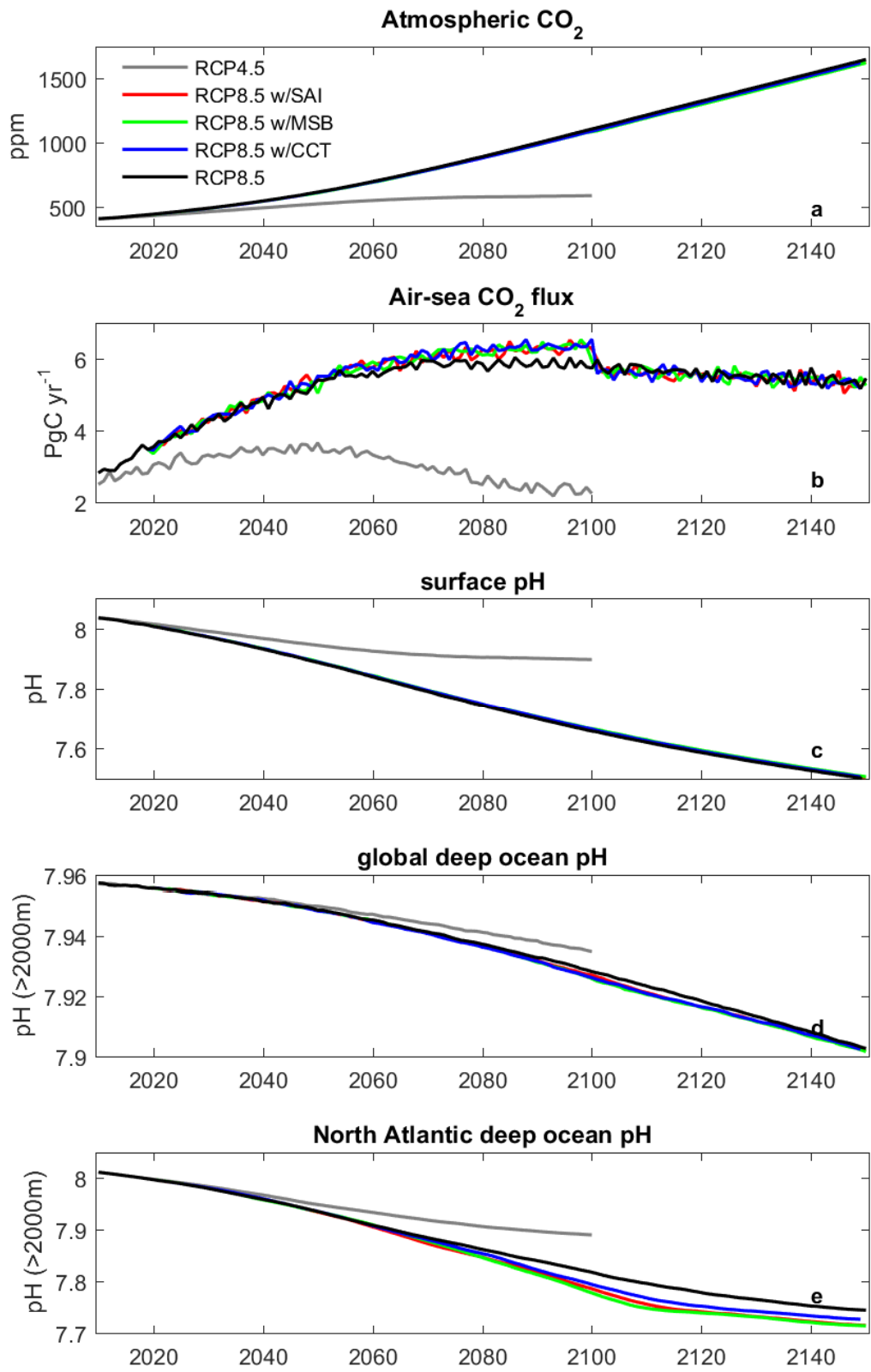
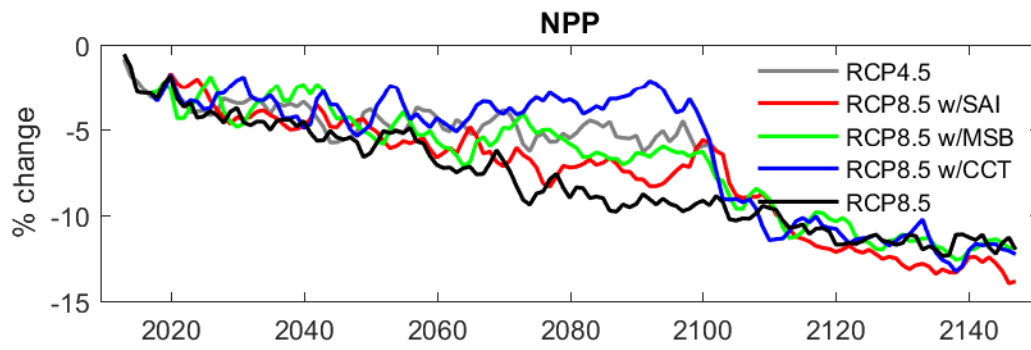
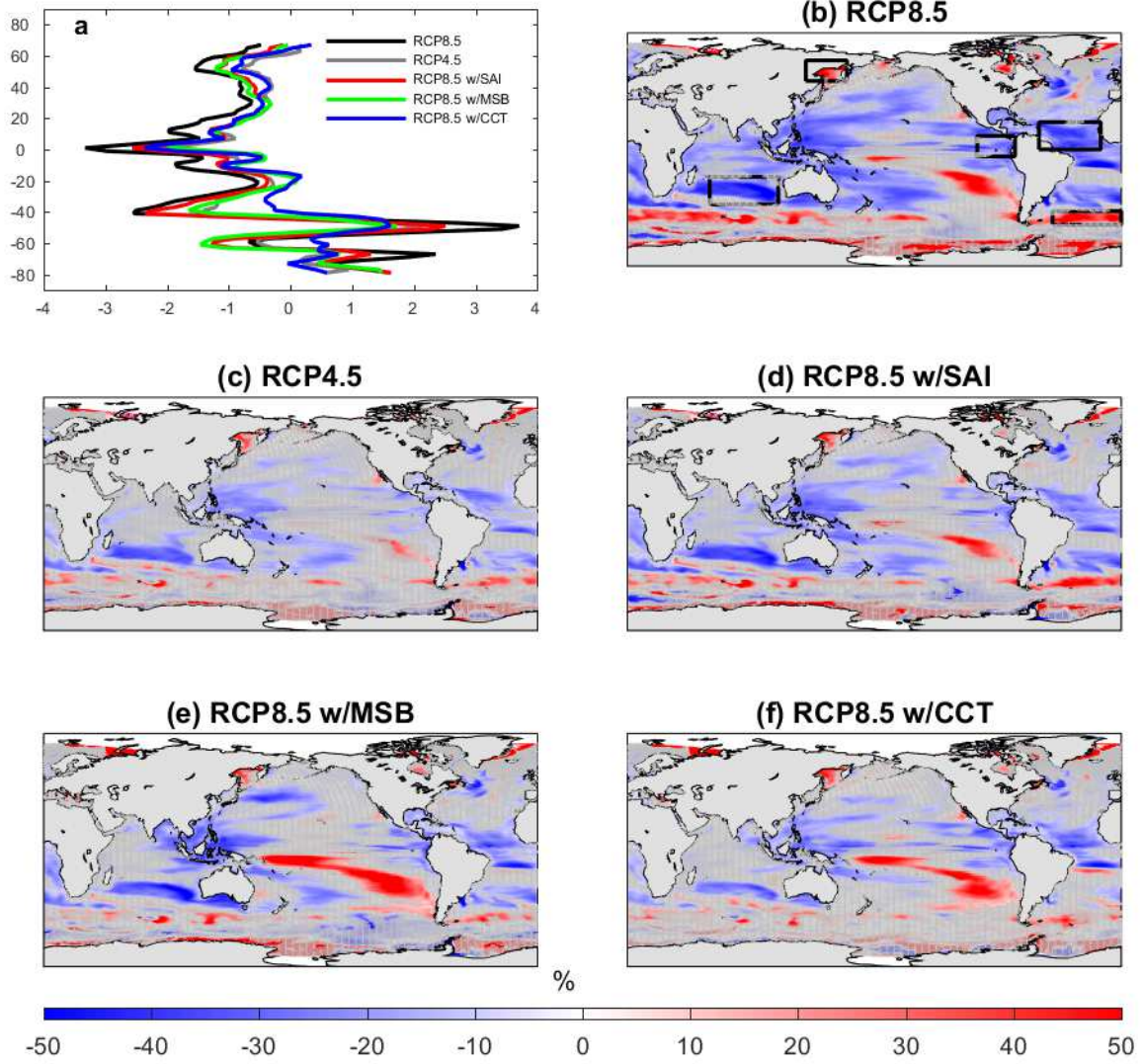


Figure 4



885 **Figure 5**

886



887 **Figure 6**

888

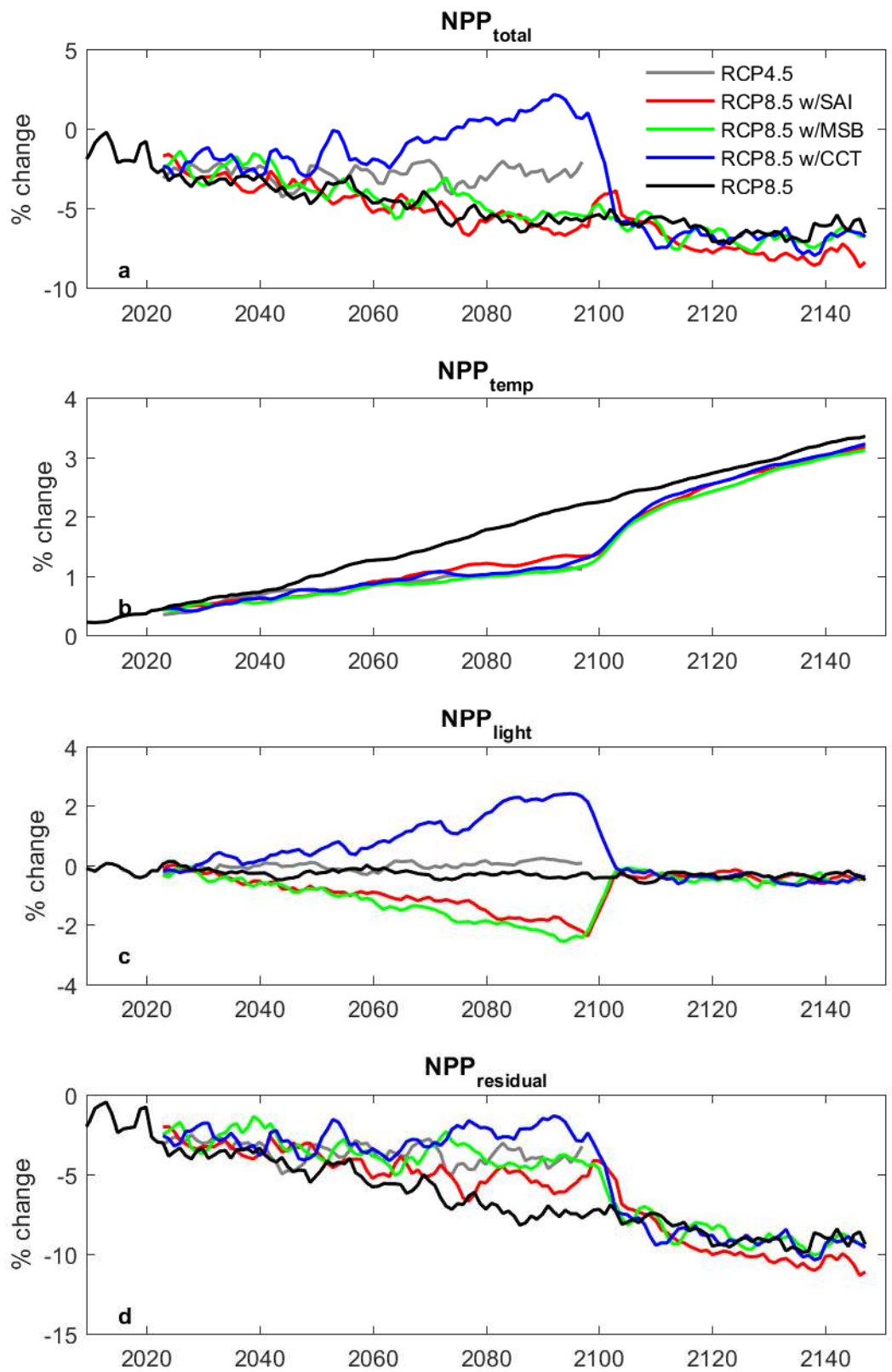
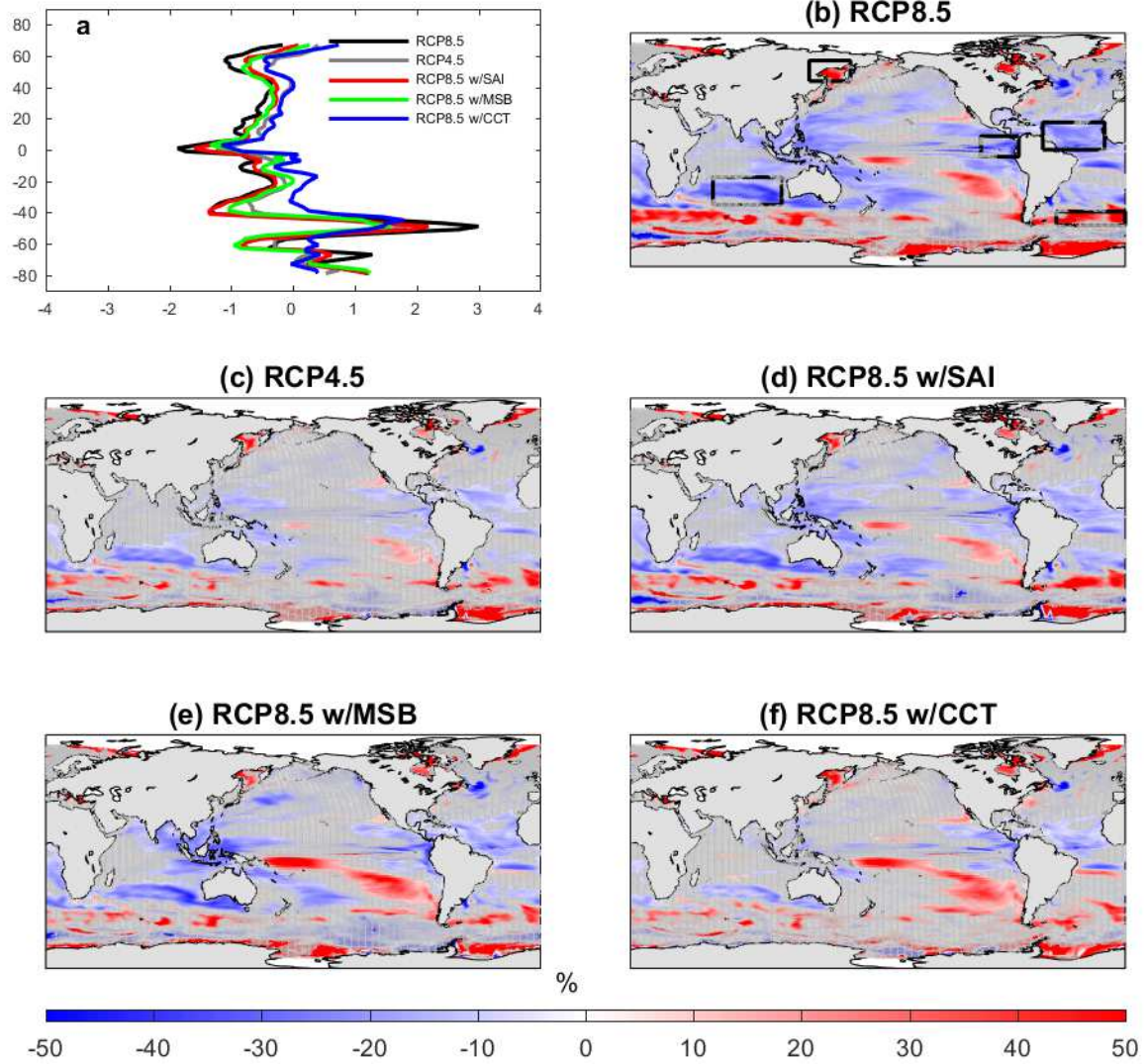


Figure 7



890 **Figure 8**

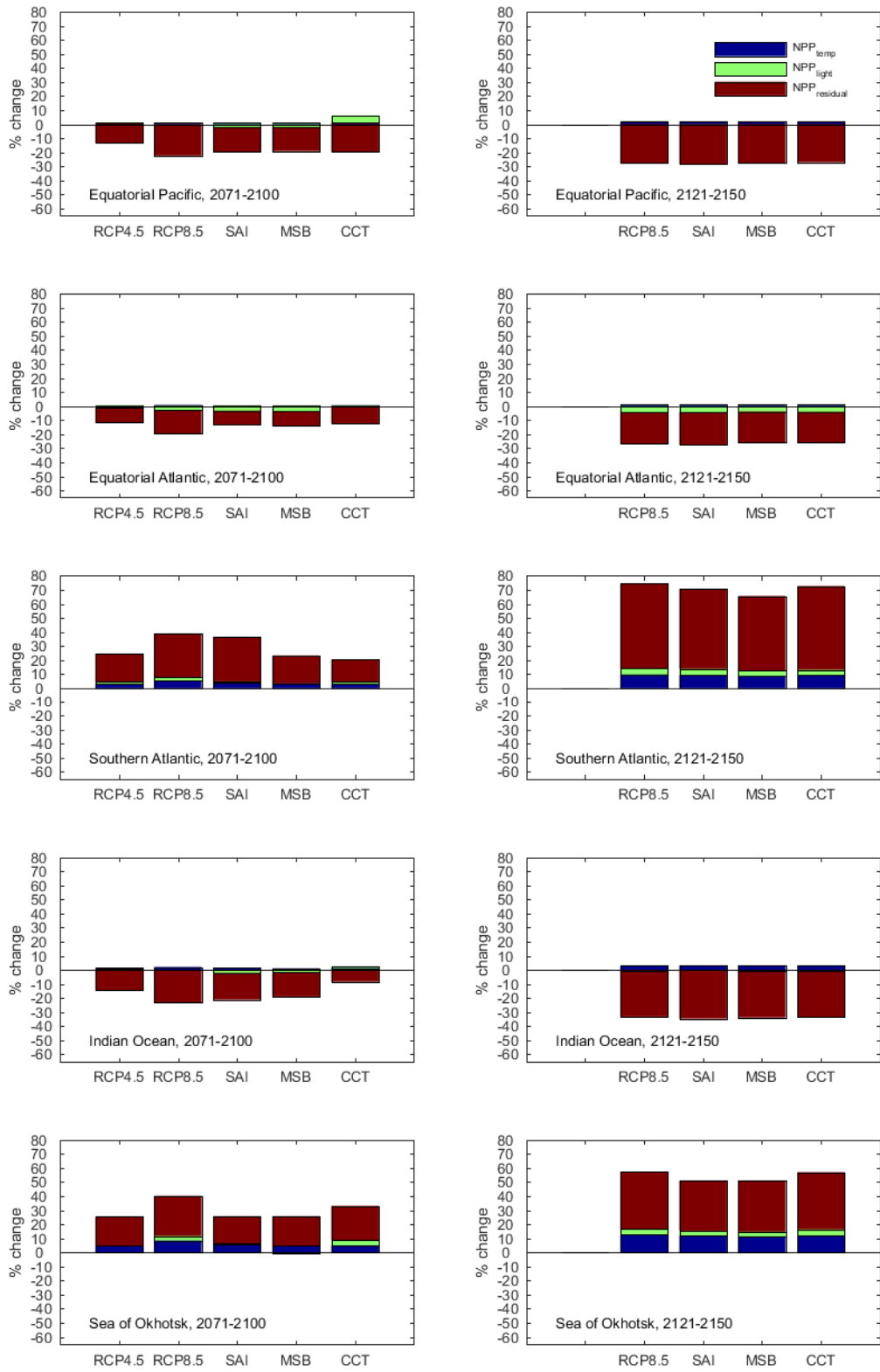


Figure 9